PARAMETRIC FILTERS FOR NON-STATIONARY INTERFERENCE MITIGATION IN AIRBORNE RADARS

Peter Parker and A. Lee Swindlehurst

Dept. of Electrical & Computer Engineering
Brigham Young University
Provo, UT 84602
{parkerp,swindle}@ee.byu.edu

ABSTRACT

Multichannel parametric filters are currently being studied as a means of reducing the dimension of STAP algorithms for interference rejection in airborne pulsed-Doppler radar systems. These filters are attractive to use due to the low computational cost associated with their implementation as well as their near optimal performance with a small amount of training data for a stationary environment. However, these filters do not perform well in certain types of non-stationary environments. This paper presents two modifications to the Space-Time AutoRegressive (STAR) filter that we previously proposed. The first modification is based on the Extended Sample Matrix Inversion (ESMI) technique and is used in the presence of range varying clutter which arises from the use of non-linear antenna arrays or bistatic radar systems. The second modification to the STAR filter is for use in the presence of hot clutter and is a three-dimensional STAP algorithm. Using a realistic simulated data set for circular array STAP, we show that the modifications to the STAR filter improve the performance when in the presence of the non-stationary interference.

1. INTRODUCTION

The use of space-time adaptive processing (STAP) for airborne radar interference mitigation is usually limited by the lack of stationary secondary data used for training the filter. This problem is made worse when the radar platform is operating under circumstances that lead to additional non-stationary components to the interference. Such circumstances include the use of a non-linear or non-side-looking array which leads to a range variation of the clutter statistics or the presence of an airborne jamming source which leads to hot clutter or terrain scattered interference.

Partially adaptive STAP filters alleviate this problem to a degree by taking advantage of the low-rank nature of the clutter. The partially adaptive STAP filters use fewer degrees of freedom and therefor need fewer training samples than the fully adaptive STAP filter. One such partially adaptive STAP filter that is discussed in this paper is the Space-Time AutoRegressive (STAR) filter [1]. The partially adaptive STAP filters offer an improvement over the fully adaptive STAP filter but are still derived based upon the assumption that the interference is stationary. When the non-stationary component of the interference follows a specified model, this model may be taken into account to derive a filter to cancel the non-stationary interference. A few partially adaptive STAP algorithms have been derived to account for range-varying interference [2] and hot clutter [3].

Parametric filters (such as the STAR filter) have been shown to achieve near optimal performance with a small amount of training data when the interference is stationary [4]. However, the performance when the interference is non-stationary leaves much room for improvement. In this paper, two extensions of the STAR filter to account for both range-varying interference and hot clutter are presented. The improvements that the range-varying Extended STAR (ESTAR) filter offers over the standard STAR filter is illustrated with a synthetic data set generated by MIT Lincoln Laboratory that simulates the output of a 20 element antenna array whose elements lie along a circular arc of 120° [2]. This ESTAR filter is also shown to have better performance than a range-varying extended post-Doppler algorithm.

The three-dimensional STAR filter used to mitigate hot clutter is tested using the same data set as above augmented with synthetic hot clutter. The 3D-STAR filter achieves a significant improvement in signal-to-interference plus noise ratio (SINR) over the standard STAR approach. In comparing the 3D-STAR filter to a three-dimensional optimized pre-Doppler algorithm, it is shown that the performance of the two filters are nearly the same but that the 3D-STAR filter has a narrower clutter notch. This narrow clutter notch allows for improved detection of slowly moving targets.

In the next section, we briefly present the standard data model used for STAP problems and introduce the notation used throughout the paper. The STAR filtering technique is described in Section 3 as a background for the extensions presented herein. Section 4 presents the range-varying extended STAR filter that is used when the clutter statistics are range-varying. Section 5 derives a 3D-STAR filter used for the mitigation of hot clutter and Section 6 shows the results of several numerical simulations of the filters.

2. DATA MODEL

A target present in a particular range bin during some coherent processing interval (CPI) may be modeled as producing the following baseband vector signal (after pulse compression and demodulation) [5]:

$$\mathbf{x}_\ell(t) = b\mathbf{a}(\theta)e^{j\omega t} + \mathbf{n}_\ell(t) \in \mathbb{C}^m, \qquad t = 1, \cdots, N, \quad (1)$$

where ℓ is the range bin in which the target is located, b is the complex amplitude of the signal, ω is the Doppler shift due to the

This work was supported by the Office of Naval Research under contract N00014-00-1-0338.

relative motion between the array platform and the target, $\mathbf{a}(\theta)$ is the response of the array to a unit amplitude plane wave arriving from direction θ (azimuth and elevation angles), and $\mathbf{n}_\ell(t)$ contains contributions from clutter, jamming, and thermal noise. In (1), we are assuming an array of m elements and a total of N transmitted pulses covering R range bins.

If we stack the N array outputs into a single $mN \times 1$ space-time snapshot, we may re-write (1) as

$$\chi_\ell = \begin{bmatrix} \mathbf{x}(1) \\ \vdots \\ \mathbf{x}(N) \end{bmatrix} = b\mathbf{s}(\theta,\omega) + \eta \qquad (2)$$

where

$$\begin{aligned} \mathbf{s}(\theta,\omega) &= \mathbf{v}(\omega) \otimes \mathbf{a}(\theta) \\ \mathbf{v}(\omega) &= \begin{bmatrix} 1 & e^{j\omega} & \cdots & e^{j(N-1)\omega} \end{bmatrix}^T \\ \eta &= \begin{bmatrix} \mathbf{n}(1)^T & \cdots & \mathbf{n}(N)^T \end{bmatrix}^T \end{aligned}$$

and $\otimes$ represents the Kronecker product. The vector η_ℓ contains the stacked vector samples of the clutter and interference for range bin ℓ, and has an unknown covariance matrix denoted by

$$\mathcal{E}\{\eta_\ell \eta_\ell^*\} = \mathbf{R} .$$

The clutter is neither temporally nor spatially white; in fact, the rank of $\mathbf{R}$ is typically much less than mN. The rank (ρ) of $\mathbf{R}$ is important because it determines how many secondary data samples are required to accurately estimate $\mathbf{R}$. According to [6], the number of required samples is on the order of 2ρ to 5ρ. The fully adaptive approach to whitening this type of data is to multiply the data by the inverse square-root of an estimate of the matrix $\mathbf{R}$. Because the size of this matrix can become quite large, its low rank nature is exploited to derive reduced-dimension whitening algorithms. The next section summarizes the work in [1] as a background for extending the STAR filter.

3. SPACE-TIME AUTOREGRESSIVE FILTERING

Following the derivation in [1], the STAR approach assumes that a set of L matrices $\mathbf{H}_0, \mathbf{H}_1, \cdots, \mathbf{H}_{L-1}$ of dimension $m' \times m$ exist that satisfy

$$\sum_{i=0}^{L-1} \mathbf{H}_i \mathbf{n}(t+i) = 0 , \quad t = 1, \cdots, N-L+1, \qquad (3)$$

for the interference and clutter in the primary range bin. We may also write (3) in the following two different ways:

$$\underbrace{[\mathbf{H}_0 \cdots \mathbf{H}_{L-1}]}_{\mathbf{H}^*} \underbrace{\begin{bmatrix} \mathbf{n}(1) & & \mathbf{n}(N-L+1) \\ \vdots & \cdots & \vdots \\ \mathbf{n}(L) & & \mathbf{n}(N) \end{bmatrix}}_{\mathbf{N}} = 0 \qquad (4)$$

or

$$\mathcal{H}^* \eta = 0 , \qquad (5)$$

where

$$\mathcal{H}^* = \begin{bmatrix} \mathbf{H}_0 & \cdots & \mathbf{H}_{L-1} & & & \\ & \mathbf{H}_0 & \cdots & \mathbf{H}_{L-1} & & \\ & & \ddots & & \ddots & \\ & & & \mathbf{H}_0 & \cdots & \mathbf{H}_{L-1} \end{bmatrix} . \qquad (6)$$

In cases where the clutter is stationary, we assume that equations (4) and (5) also hold for the secondary data as well:

$$\begin{aligned} \mathbf{H}^* \mathbf{N}_k &= 0 \qquad (7) \\ \mathcal{H}^* \eta_k &= 0 , \qquad (8) \end{aligned}$$

for $k = 1, \cdots, N_s$, where N_s is the number of secondary data snapshots used to train the filter.

The matrix $\mathcal{H}$ is $mN \times m'(N-L+1)$. If (3) holds and m' and L are chosen so that $m'(N-L+1)$ is large enough, the columns of $\mathcal{H}$ form a basis for the space orthogonal to the clutter and interference subspace. Although this relationship does not hold in practice due to the presence of thermal noise, a least squares solution is applied to approximate the subspace. This suggests the following space-time filter (similar to the matched subspace detectors in [7]) be used for interference rejection:

$$\mathbf{w}_{AR}(\theta,\omega) = \mathbf{P}_{\mathcal{H}} \mathbf{s}(\theta,\omega) , \qquad (9)$$

where $\mathbf{P}_{\mathcal{H}}$ is the projection onto the columns of $\mathcal{H}$:

$$\mathbf{P}_{\mathcal{H}} = \mathcal{H} (\mathcal{H}^* \mathcal{H})^{-1} \mathcal{H}^* . \qquad (10)$$

We refer to the implementation of STAP with the weight vector of (9) as Space-Time AutoRegressive (STAR) filtering. The STAR filter weights are "adaptive" in the sense that $\mathcal{H}$ must be estimated from the secondary data prior to computation of $\mathbf{w}_{AR}$.

4. RANGE-VARYING EXTENDED STAR FILTER

The STAR filter of the previous section is not designed to handle non-stationary interference of any kind. This section derives a STAR-based filter that assumes the clutter statistics vary linearly with range. This assumption is reasonable if the training region is kept short. The idea of using time-varying weights in a STAP algorithm was introduced in [8] as an extended sample matrix inversion algorithm and this idea was used for range-varying STAP weights in [2]. This technique increases the dimension of the problem by a factor of two but does improve the performance when there is a rapidly changing clutter locus.

The idea behind range-varying weights is that the weight vector is a function of range (r) to account for the non-stationary clutter locus. Expanding the weight vector into a power series yields

$$\mathbf{w}(r) = \mathbf{w}_o + r\dot{\mathbf{w}}_o + \frac{r^2 \ddot{\mathbf{w}}_o}{2} + \cdots . \qquad (11)$$

The assumption is made that the clutter locus is changing slowly enough that for a given collection of ranges the weight vector is linear in r. Ignoring the higher order terms in the Taylor series, the weight vector as a function of the k^{th} range bin becomes

$$\mathbf{w}_k = \mathbf{w}_o + \alpha k \Delta \mathbf{w}_o, \qquad (12)$$

where α is a normalization constant. Defining

$$\tilde{\mathbf{w}} = \begin{bmatrix} \mathbf{w}_o \\ \Delta \mathbf{w} \end{bmatrix} \qquad (13)$$

the output of the filter may be written as

$$\mathbf{z} = \tilde{\mathbf{w}}^* \begin{bmatrix} \chi_k \\ \alpha k \chi_k \end{bmatrix} = \tilde{\mathbf{w}}^* \tilde{\chi}_k, \qquad (14)$$

where $\tilde{\chi}_k$ is the extended data vector.

Using this same idea for the STAR filter (*i.e.*, assuming that the STAR filter coefficients that null the clutter vary linearly with range) we can rewrite (3) using an extended data vector:

$$\sum_{i=0}^{L-1} \left[\begin{array}{cc} \mathbf{H}_i & \Delta\mathbf{H}_i \end{array} \right] \left[\begin{array}{c} \mathbf{n}_k(t-i) \\ \alpha k \mathbf{n}_k(t-i) \end{array} \right] = \mathbf{0}, \quad t = L{+}1, \cdots, N. \tag{15}$$

Letting $\Delta\mathbf{H}$ and $\Delta\mathcal{H}$ be defined similar to $\mathbf{H}$ in (4) and $\mathcal{H}$ in (6) we may rewrite (7) and (8) as

$$\left[\begin{array}{cc} \mathbf{H}^* & \Delta\mathbf{H}^* \end{array} \right] \left[\begin{array}{c} \mathbf{N}_k \\ \alpha k \mathbf{N}_k \end{array} \right] = 0 \tag{16}$$

$$\left[\begin{array}{cc} \mathcal{H}^* & \Delta\mathcal{H}^* \end{array} \right] \left[\begin{array}{c} \eta_k \\ \alpha k \eta_k \end{array} \right] = 0. \tag{17}$$

The filter parameters $\mathbf{H}$ and $\Delta\mathbf{H}$ may then be estimated using the left null space of the matrix

$$\tilde{\mathcal{N}} = \left[\begin{array}{ccc} \mathbf{N}_{-Q} & \cdots & \mathbf{N}_Q \\ -\alpha Q \mathbf{N}_{-Q} & \cdots & \alpha Q \mathbf{N}_Q \end{array} \right], \tag{18}$$

where $Q = \frac{N_s}{2}$. Following what was done in [2], the constant α is chosen as

$$\alpha = \sqrt{\frac{12}{(N_s+2)(N_s+1)}} \tag{19}$$

to yield a "flat" noise subspace.

To define what the weight vector is, let

$$\tilde{\mathcal{H}} = \left[\begin{array}{c} \mathcal{H} \\ \Delta\mathcal{H} \end{array} \right] \tag{20}$$

so that

$$\mathbf{w}_E(\theta,\omega) = \mathbf{P}_{\tilde{\mathcal{H}}} \left[\begin{array}{c} \mathbf{s}(\theta,\omega) \\ \mathbf{0} \end{array} \right]. \tag{21}$$

Filtering the extended data vector with (21) is referred to as the Extended STAR (ESTAR) filter. When estimating a range varying weight vector using data that also varies with range, a higher number of training vectors may be used before performance starts to degrade.

5. STAR FILTERING FOR HOT CLUTTER

When the radar platform is operating in an environment where there is an airborne jamming source present, two main considerations must be made. First, the hot clutter covariance changes from pulse to pulse and second, the hot clutter has non-zero correlations across range bins [3]. This section derives a STAR based filter that is effective in canceling hot clutter. The baseline STAR filter is first modified to handle any type of interference that changes from pulse to pulse (as with intrinsic clutter motion) and then an additional dimension is added to the vector autoregressive filter to account for the correlations across range bins.

The model for the clutter in (3) is no longer valid since the spatial covariance changes from pulse to pulse. If the standard STAR model is used in a non-stationary environment like hot clutter, it tries to account for the time variations in the data by increasing the number of filter taps required to achieve clutter cancelation. A better model for this is to let the coefficients of the space-time prediction error filter change with time:

$$\mathcal{H}_{TV}^* = \left[\begin{array}{ccccc} \mathbf{H}_0(1) & \cdots & \mathbf{H}_{L-1}(1) & & \\ & \ddots & & \ddots & \\ & & \mathbf{H}_0(n) & \cdots & \mathbf{H}_{L-1}(n) \end{array} \right], \tag{22}$$

where $n = N - L + 1$ and where each block row is a set of new coefficients based on dropping the data from the oldest pulse and adding the data from the most recent pulse. For this time-varying STAR filter, a greater number of filter parameters must be estimated (n times the degrees of freedom required for the standard STAR algorithm) and therefore, more sample support is required to train the filter.

To complete the derivation of the 3D-STAR filter, a few definitions need to be made. To clarify the notation, sampling across pulses is called slow-time sampling and sampling across range bins is called fast-time sampling. Let P be the number of fast-time samples over which the hot clutter is correlated.

In order to utilize the fast-time correlation of the data, an extra dimension is added to the STAR filter. We assume for a moment that the interference is stationary across the pulses (slow-time). This filter will model the fast-time and slow-time correlations with a two-dimensional VAR filter. For a set of LJ matrices of size $M' \times M$, assume that the clutter obeys the model

$$\sum_{j=0}^{J-1} \sum_{i=0}^{L-1} \mathbf{H}_{i,j} \mathbf{n}_{k+j}(t+i) = \mathbf{0}, \quad t = 1, \cdots, N-L+1$$
$$k = 1, \cdots, P-J+1, \tag{23}$$

where $k = 0$ is the range bin of interest and $\mathbf{n}_k(t)$ is the spatial snapshot for the t^{th} pulse and the k^{th} range bin. This may also be expressed as

$$\sum_{j=0}^{J-1} \mathcal{H}_j^* \mathbf{e}_{k+j} = \mathbf{0} \quad k = 1, \cdots, P-J+1, \tag{24}$$

where $\mathcal{H}_j$ is the matrix defined in (6) with a subscript j to indicate which fast-time sample it is associated with. From this point we again take into account the slow-time variations caused by the hot clutter by replacing $\mathcal{H}_j$ with the slow-time varying filter $\mathcal{H}_{TV,j}$.

Rewriting this sum with the time-varying filter we get

$$\mathbb{H}^* \eta_{3d}(k) = 0, \tag{25}$$

where

$$\eta_{3D}(k) = \left[\begin{array}{c} \eta_k \\ \vdots \\ \eta_{k+P-1} \end{array} \right]$$

$$\mathbb{H}^* = \left[\begin{array}{ccccc} \mathcal{H}_{TV,0}^* & \cdots & \mathcal{H}_{TV,J-1}^* & & \\ & \ddots & & \ddots & \\ & & \mathcal{H}_{TV,0}^* & \cdots & \mathcal{H}_{TV,J-1}^* \end{array} \right].$$

Assuming that there is target energy in the $k = 0$ range bin, then there will also be target energy in the vectors $\eta_{3d}(0)$, $\eta_{3d}(-1)$, $\cdots$, $\eta_{3d}(-P+1)$ which may not be used for training the filter. In

order to define the algorithm to find the filter coefficients let

$$\tilde{\mathbf{H}}(t)^* = [\ \mathbf{H}_{0,0}(t) \ \cdots \ \mathbf{H}_{L-1,J-1}(t)\ ] \quad (26)$$

$$\mathbf{g}_k(t) = \begin{bmatrix} \mathbf{n}_k(t) \\ \vdots \\ \mathbf{n}_k(t+L-1) \end{bmatrix} \quad (27)$$

$$\mathcal{G}_k(t) = \begin{bmatrix} \mathbf{g}_k(t) & \cdots & \mathbf{g}_{k+P-J}(t) \\ \vdots & & \vdots \\ \mathbf{g}_{k+J-1}(t) & \cdots & \mathbf{g}_{k+P-1}(t) \end{bmatrix} \quad (28)$$

$$\mathbf{G}(t) = [\ \mathcal{G}_1(t) \ \cdots \ \mathcal{G}_{N_s}(t)\ ]. \quad (29)$$

The filter coefficients can then be found by the following least squares criterion:

$$\hat{\tilde{\mathbf{H}}}(t) = \arg\min_{\tilde{\mathbf{H}}(t)} \left\| \tilde{\mathbf{H}}(t)^* \mathbf{G}(t) \right\|_F^2 \quad t = 1, \cdots, N-L+1 \quad (30)$$

subject to the constraint that $\mathbf{H}(t)^*\mathbf{H}(t) = \mathbf{I}$. From this point the m' left singular vectors corresponding to the smallest singular values of each $\mathbf{G}(t)$ matrix will be used to compute the $N-L+1$ sets of filter coefficients which define $\mathbf{H}$. With a defined subspace, a weight vector for mitigation of hot clutter is

$$\mathbf{w}_{3D}(\theta,\omega) = \mathbf{P}_{\mathbf{H}}\mathbf{s}_{3D}(\theta,\omega), \quad (31)$$

where

$$\mathbf{s}_{3D}(\theta,\omega) = \begin{bmatrix} 1 \\ 0 \\ \vdots \\ 0 \end{bmatrix} \otimes \mathbf{s}(\theta,\omega). \quad (32)$$

This 3D-STAR filter will require more training data than the STAR filter (on the order of $N-L+1$ times more) due to the non-stationary prediction error filter that is used in the implementation. This additional sample support requirement is less of an issue than with other 3D implementations because the STAR approach typically requires much less secondary data for good performance. The 3D-STAR filter also assumes that the data is stationary for P fast-time samples.

6. NUMERICAL RESULTS

The algorithms presented herein are tested using a data set created by MIT Lincoln Laboratory that simulates the output of a 20 element array. These elements lie along a circular arc of 120° with radius 2.96m and are assumed to have a cosine-shaped response with a -30 dB backlobe for both azimuth and elevation dimensions. The airborne platform is moving with a velocity of 100 m/s above a 4/3 eath model at an altitude of 9000m. The operating frequency of the radar is taken to be 435 MHz, the radar bandwidth and sampling frequency are 3.75 MHz, the pulse-repetition frequency is 300 Hz, and $N = 18$ pulses are assumed to be transmitted during one CPI. Data are generated for 9325 range gates between 20 and 400 km with a clutter-to-white-noise power ratio of 40 dB at a range of 100km.

Hot clutter is included in the data by adding a term of the form

$$\mathbf{j}_k = b_j \begin{bmatrix} \mathbf{c}_k(1) \\ \vdots \\ \mathbf{c}_k(N) \end{bmatrix},$$

where b_j is the amplitude of the jammer,

$$\mathbf{c}_k(t) = \mathbf{a}(\theta_j)z_k + \sum_{i=1}^{\ell} \mathbf{b}(t)z_{k-i}$$

is the contribution of the hot clutter for a single pulse at range k, ℓ is the longest multipath delay, θ_j is the direction of arrival of the jammer signal, z_k is the jammer waveform (white in both slow and fast-time), and $\mathbf{b}_t$ is a random vector that approximates the sum of the spatial steering vectors for each of the multipath signals. When present, the jammer-to-clutter power ratio is assumed to be 10 dB. When secondary data are used to estimate the clutter covariance or STAR filter parameters, equal amounts of data from range bins on either side of the target range bin are used.

The true clutter covariance matrix used to generate the data is known for 20 of the 9325 range bins, and thus the maximum achievable SINR can be calculated at these ranges. To illustrate the performance of the algorithms we use either the SINR loss as a function of Doppler for an azimuth of 0° or the "average" SINR loss as compared with the optimal (known covariance) solution. This average SINR loss is defined as the area between the algorithm's SINR curve and that achievable assuming $\mathbf{R}$ is known. This is depicted in Figure 1. The ESTAR filter will be compared to the range-varying extended post-Doppler PRI staggered STAP algorithm [2] and the 3D-STAR algorithms will be compared with the optimized 3D pre-Doppler STAP algorithm [3]. For the STAR based filters, $M' = 20$ is used for all the examples and for the partially adaptive STAP algorithm, three pulses at a time are processed and a diagonal loading of about five times the noise level is used for sample matrix inversion.

A performance evaluation of the ESTAR filter at a range of 20km is shown in Figures 2 and 3. Figure 2 compares the performance of the ESTAR filter and the basic STAR filter as a function of L for $N_s = 50$ (2km training window). This figure shows that the ESTAR filter does perform better than the STAR filter at close ranges. We also see that the ESTAR filter requires fewer filter taps than the STAR filter thus offsetting some of the additional computational cost associated with the extended implementation. Figure 3 compares the performance of the STAR filters with the range-varying extended PRI staggered and fully adaptive STAP algorithms as a function of training length. Note that the performance of the STAR algorithm degrades quickly as more training data is used. The extended PRI STAP and ESTAR filters both have nearly flat performance as N_s is increased due to the range-varying weights. The ESTAR filter also has much better performance than the extended PRI STAP algorithm because it requires much less training data to converge to its best performance.

Another aspect of performance is the computational load required to implement the algorithms. For the STAR algorithms the implementation is broken up into two steps. The first step involves taking the SVD of the $2ML \times (N-L+1)N_s$ data matrix $\tilde{\mathcal{N}}$ and the second is forming the projection operator. The bulk of the computation involved in this second step is finding the inverse of $\tilde{\mathcal{H}}^*\tilde{\mathcal{H}}$ which is usually a sparse banded matrix. Taking this into account the computational load for the ESTAR algorithm is

$$O(4(ML)^2(N-L+1)N_s) + O((ML)^2(N-L+1)M').$$

For the parameters of the circular array data with $L = 4$ and $M' = 20$, the computational cost is

$$\text{ESTAR} = O(3.84 \times 10^5 N_s) + O(1.92 \times 10^6).$$

Comparing this with the cost of the STAR filter (at $L = 5$):

$$\begin{aligned} \text{STAR} &= O((ML)^2(N-L+1)N_s) \\ &\quad +O((ML)^2(N-L+1)M') \\ &= O(1.4\times 10^5 N_s) + O(2.8\times 10^6) \end{aligned}$$

the ESTAR algorithm has only a small increase in computational load. The extended PRI STAP algorithm has a computational cost of

$$\begin{aligned} \text{EPRISTAP} &= O(4(MK)^2(N-K+1)N_s) \\ &\quad +O(4(MK)^2(N-K+1)\rho) \\ &= O(2.3\times 10^5 N_s) + O(2.0\times 10^7) \end{aligned}$$

where $K = 3$ pulses that are processed at a time and $\rho = 90$ is the approximate rank of each sub-CPI. From this we see that if N_s is not too big ($N_s < 100$), then the ESTAR algorithm requires much fewer computations than the PRI-staggered STAP algorithm.

Figures 4-6 illustrate the performance of the 3D-STAR filter when there is hot clutter present and when the direct path jamming signal is in the mainbeam of the radar system. Figure 4 compares the performance of the 3D-STAR filter to the basic STAR filter as a function of L. The 3D-STAR filter outperforms the STAR filter with a small number of filter taps by utilizing the slow-time-varying taps as well as the additional fast time tap. Figure 5 compares the STAR filters to the 3D optimized pre-Doppler and fully adaptive STAP algorithms as a function of training data. In this case the pre-Doppler and 3D-STAR algorithms have a very similar performance with the pre-Doppler algorithm slightly outperforming the 3D-STAR filter. However, Figure 6, which shows the SINR at $N_s = 80$ or 3.2 km, illustrates that the 3D-STAR filter has a narrower clutter notch which results in a lower detectable velocity. If the small loss in performance away from the clutter notch is tolerable, the 3D-STAR filter is more desirable due to its greater percentage of usable Doppler space.

The computational cost of the STAR ($L = 7$), 3D-STAR ($L = 2$, $J = 2$), and 3D-pre Doppler ($K = 3$ pulses) algorithms for the system parameters described above are as follows:

$$\text{STAR} = O(2.35\times 10^5 N_s) + O(4.7\times 10^6)$$

$$\begin{aligned} \text{3D}-\text{STAR} &= O((MLJ)^2(N-L+1)(P-J+1)N_s) \\ &\quad +O((MLJ)^2(N-L+1)(P-J+1)M') \\ &= O(2.18\times 10^5 N_s) + O(4.35\times 10^6) \end{aligned}$$

$$\begin{aligned} \text{pre}-\text{Dopp} &= O((MKP)^2(N-K+1)N_s) \\ &\quad +O((MKP)^2(N-K+1)\rho) \\ &= O(5.18\times 10^5 N_s) + O(7.0\times 10^7) \end{aligned}$$

where $\rho = 135$ is the approximate rank of the sub-CPI covariance matrix. Again we see that the STAR and 3D-STAR algorithms have nearly the same computational cost when the filter orders are chosen close to the best value. It is also seen that the pre-Doppler algorithm requires a large number of computations when compared with the 3D-STAR algorithm.

7. CONCLUSIONS

This paper has presented modifications to the space-time autoregressive (STAR) filter for two types of non-stationary interference. The first modified filter (ESTAR) is used when the clutter statistics are varying with range as is the case for non-linear antenna arrays or bistatic radar systems. The second modification (3D-STAR) is used in the presence of hot clutter which arises when an airborne jamming source is present. These two modifications provide an increase in performance over the standard STAR filter when used in non-stationary environments without a major increase in computational burden. We have shown in numerical experiments and computational analysis that the ESTAR filter is superior to the extended PRI-staggered post-Doppler STAP algorithm when there is a rapidly changing clutter locus. We have also shown that the 3D-STAR filter has a little more usable Doppler space than the 3D optimized pre-Doppler STAP algorithm and the 3D-STAR algorithm achieves this performance with much less computation.

8. REFERENCES

[1] A. L. Swindlehurst and P. Parker, "Parametric clutter rejection for space-time adaptive processing," in *Proc. of the ASAP-2000 Workshop*, (MIT Lincoln Laboratory, Lexington, MA), 2000.

[2] M. Zatman, "Circular array STAP," *IEEE Trans. on Aerospace and Electronic Systems*, vol. 36, pp. 510–517, April 2000.

[3] D. J. Rabideau, "Clutter and jammer multipath cancellation in airborne adaptive radar," *IEEE Trans. on Aerospace and Electronic Systems*, vol. 36, pp. 565–583, April 2000.

[4] J. Román, D. Davis, and J. Michels, "Multichannel parametric models for airborne phased array clutter," in *Proc. IEEE Radar Conf.*, vol. 1, (Syracuse, NY), pp. 72–77, 1997.

[5] J. Ward, "Space-time adaptive processing for airborne radar," Tech. Rep. TR-1015, MIT Lincoln Labs, Dec 1994.

[6] I. S. Reed, J. D. Mallett, and L. E. Brennan, "Rapid convergence rate in adaprive arrays," *IEEE Trans. on Aerospace and Electronic Systems*, vol. AES-10, pp. 853–863, Nov 1974.

[7] L. Scharf and B. Friedlander, "Matched subspace detectors," *IEEE Trans. on Sig. Proc.*, vol. 42, pp. 2146–2157, August 1994.

[8] S. D. Hayward, "Adaptive beamforming for rapidly moving arrays," in *Int. Conf. on Radar*, (Beijing), pp. 480–483, CIE, Oct. 1996.

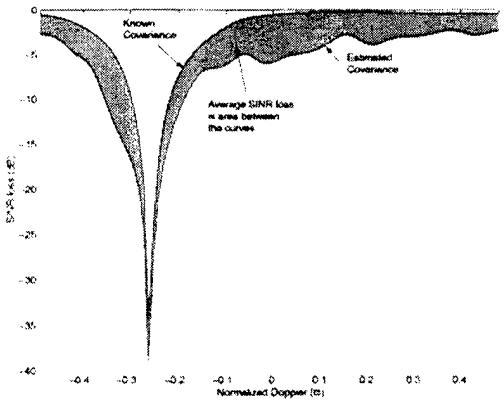

Figure 1: Definition of average SINR loss for a particular algorithm.

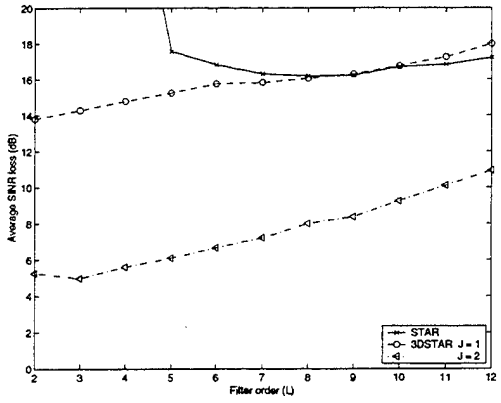

Figure 4: Performance of STAR filters as a function of filter order with hot clutter present.

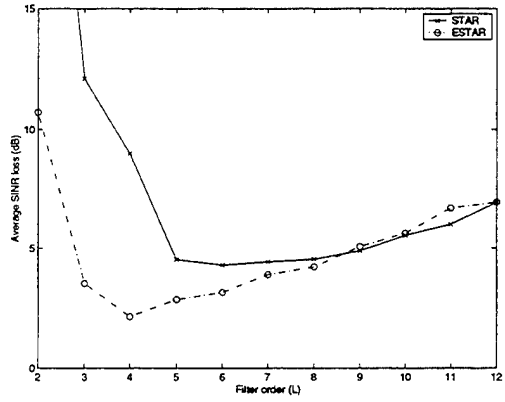

Figure 2: Performance of ESTAR and STAR at 20 km as a function of filter order.

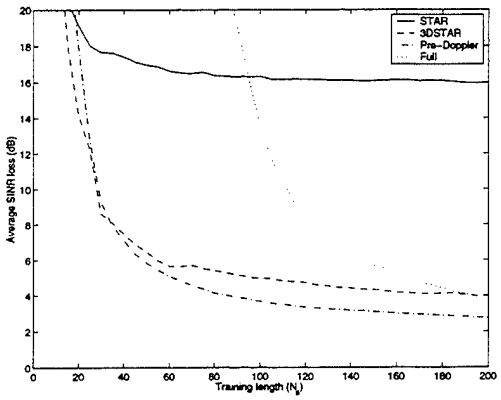

Figure 5: Convergence of STAR, 3D-STAR, pre-Doppler, and fully adaptive algorithms with hot clutter present.

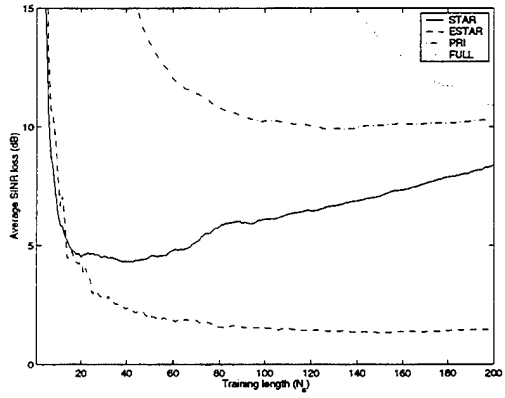

Figure 3: Comparison with PRI-Staggered and fully adaptive STAP at 20 km as a function of training length

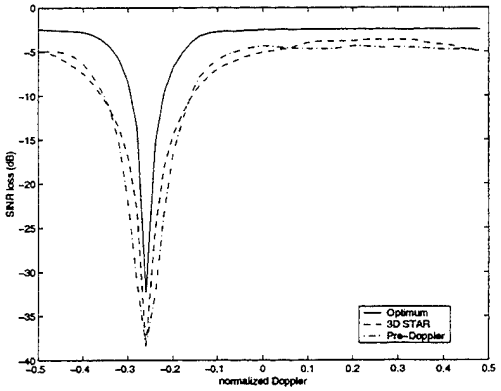

Figure 6: SINR of 3D-STAR and pre-Doppler algorithms with $N_s = 80$ and hot clutter present.